Influence of Non-Uniform Distributions of Filler Porosity on the Thermal Performance of Thermocline Storage Tanks

YUCHAO HUA, LINGAI LUO
CNRS, Laboratoire de thermique et énergie de Nantes
Nantes Université
La Chantrerie, Rue Christian Pauc, 44300 Nantes
FRANCE

Abstract: -Thermal energy storage is of critical importance for the highly-efficient utilization of renewable energy sources. Over the past decades, the single-tank thermocline technology has attracted much attention owing to its high cost-effectiveness. In the present work, we investigate the influence of the filler porosity's non-uniform distribution on the thermal performance of the packed-bed sensible heat thermocline storage tanks, using the analytical model obtained by the Laplace transform. Our analyses prove that the different porosity distributions can result in the significantly different behaviors of outlet temperature and thus the varied charging and discharging efficiencies, when the total amount of filler materials (i.e., the integration of porosity) is fixed. The results indicate that a non-uniform distribution of the fillers with the proper design can improve the heat storage performance without changing the total amount of the filling materials, which may provide a new way to optimize the thermocline storage tanks.

Key-Words: - Energy storage, Heat thermocline tank, Packed bed, Transient thermal analysis, Analytical model, Laplace transform, Solar energy

Received: August 15, 2021. Revised: June 19, 2022. Accepted: July 17, 2022. Published: August 5, 2022.

1 Introduction

The utilization of renewable energy sources serves as the key solution for the problems from carbon emission to environment pollution. In this regard, the solar energy has shown its feasibility for various industrial and domestic applications [1]. Due to the strong time dependence of solar irradiation, the integration of thermal energy storage (TES) modules plays the crucial role for the solar plants, which allows the power output be flexible and stable [2][3]. Therefore, the performance of TES is of critical importance for the overall efficiency of solar plants [4].

Among the existing thermal energy storage technologies, the single-tank thermocline tank [5], where both the hot and cold fluids are contained in a single tank, has received much attention due to its high cost-effective approach compared to the conventional two-tank storage systems. For a thermocline tank, some inexpensive solid materials are usually filled into it to reduce the volume of expensive heat transfer fluid (HTF) required for storage and improve the degree of thermal stratification [6]. The research on the influence of the filler's properties, like material types, porosity and thermal conductivity etc., has been extensively investigated in literature [6–9]. Nevertheless, the filler distribution within the thermocline tank is usually assumed to be uniform. Few research papers have well discussed the effect of non-uniform distributions of filler on the performance of thermocline storage tanks.

The present work is to study the packed-bed sensible heat thermocline tanks with the filler of non-uniform distribution. An analytical model is derived by the Laplace transform, which is capable of considering the non-uniform distribution of filler porosity. Based on this model, it is found that the different porosity distributions can led to the significantly different behaviors of outlet temperature of HTF when the total amount of filler materials is fixed.

2 Problem Formulation

Fig. 1 illustrates a typical thermocline heat storage tank with height H and diameter $2R$. Here, different

from the previous work, the porosity distribution of filler is non-uniform and assumed to be dependent on the height of tank.

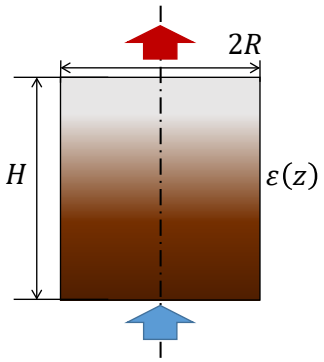

Fig. 1 Schematic of the thermocline heat storage tank during the discharging process.

To construct the governing equations, a set of assumptions are adopted as follows:

(a) The distributions of fluid flow and solid filler are assumed to be uniform in radial direction, and thus the problem becomes one dimensional along the axil direction;
(b) The heat conduction within packed bed along axil direction is neglected;
(c) The flow is assumed to be incompressible and laminar.

Therefore, the transient thermal transport process within a specific packed-bed sensible heat thermocline storage tank for discharging is governed by the 1D equations for the heat transfer fluid and the solid filler respectively,

$$\varepsilon(z)\rho_{\mathrm{f}}C_{\mathrm{f}}\frac{\partial T_{\mathrm{f}}}{\partial t}+\varepsilon(z)\rho_{\mathrm{f}}C_{\mathrm{f}}U(z)\frac{\partial T_{\mathrm{f}}}{\partial z}= h_{\mathrm{fs}}(z)a_{\mathrm{fs}}(z)(T_{\mathrm{s}}-T_{\mathrm{f}})+h_0a_0(T_0-T_{\mathrm{f}}) \quad (1)$$

$$\big(1-\varepsilon(z)\big)\rho_{\mathrm{s}}C_{\mathrm{s}}\frac{\partial T_{\mathrm{s}}}{\partial t}= -h_{\mathrm{fs}}(z)a_{\mathrm{fs}}(z)(T_{\mathrm{s}}-T_{\mathrm{f}})+h_0a_0(T_0-T_{\mathrm{s}}) \quad (2)$$

in which $\varepsilon(z)$ is the porosity of the packed-bed fillers, $T_{\mathrm{f(s)}}$ is the temperature of fluid "f" and solid "s", $\rho_{\mathrm{f(s)}}$ is the density, $C_{\mathrm{f(s)}}$ is the specific heat, $U(z)$ is the fluid velocity, h_0 is the effective heat transfer coefficient (HTC) for heat loss to the ambient of temperature T_0, and a_0 is the area per unit length for the ambient heat loss. The heat transfer surface area of fillers per unit length a_{fs} is

$$a_{\mathrm{fs}}(z)=\frac{6\big(1-\varepsilon(z)\big)\pi R^2}{d} \quad (3)$$

with the equivalent diameter of filler particles d. Moreover, the HTC, $h_{\mathrm{fs}}(z)$, between fluid and solid in porous media is given by [9],

$$h_{\mathrm{fs}}=0.191\frac{\dot{m}C_{\mathrm{f}}}{\varepsilon\pi R^2}Re^{-0.278}Pr^{-2/3} \quad (4)$$

where $\dot{m}$ is the mass flow rate, Pr is the Prandtl number, and the Reynolds number (Re) is modified for porous media as [6],

$$Re=\frac{4\dot{m}}{\varepsilon\pi R^2\mu_{\mathrm{f}}}\frac{\varepsilon d}{4(1-\varepsilon)} \quad (5)$$

with the fluid dynamic viscosity μ_{f}.

Here, the porosity ε is set as a function varying with the height of the storage tank (z), which corresponds to the non-uniform distributions of filling materials. The average porosity $\bar{\varepsilon}$ of the fillers is calculated as,

$$\bar{\varepsilon}=\frac{\int_0^H\varepsilon(z)dz}{H} \quad (6)$$

Then, the average fluid velocity is given by,

$$\bar{U}=\frac{\dot{m}}{\rho_{\mathrm{f}}\bar{\varepsilon}\pi R^2}. \quad (7)$$

For clarity, the governing equations (1) & (2) are converted to be dimensionless:

$$\frac{\partial\theta_{\mathrm{f}}}{\partial t^*}=\frac{1}{\tau_{\mathrm{fs}}}(\theta_{\mathrm{s}}-\theta_{\mathrm{f}})-\frac{U}{\bar{U}}\frac{\partial\theta_{\mathrm{f}}}{\partial z^*}+\frac{1}{\tau_0}(\theta_0-\theta_{\mathrm{f}}), \quad (8)$$

$$\frac{\partial\theta_{\mathrm{s}}}{\partial t^*}=-\frac{\mathrm{HCR}}{\tau_{\mathrm{fs}}}(\theta_{\mathrm{s}}-\theta_{\mathrm{f}})-\frac{\mathrm{HCR}}{\tau_0}(\theta_{\mathrm{s}}-\theta_0), \quad (9)$$

with the dimensionless numbers as below,

$$z^*=\frac{z}{H},t^*=\frac{\bar{U}t}{H},$$

$$\theta_{\mathrm{f}}=\frac{T_{\mathrm{f}}-T_c}{T_h-T_c},\theta_{\mathrm{s}}=\frac{T_{\mathrm{s}}-T_c}{T_h-T_c},\theta_0=\frac{T_0-T_c}{T_h-T_c},$$

$$\tau_{\mathrm{fs}}=\frac{\bar{U}}{H}\frac{\varepsilon\rho_{\mathrm{f}}C_{\mathrm{f}}}{h_{\mathrm{fs}}a_{\mathrm{fs}}},\tau_0=\frac{\bar{U}}{H}\frac{\varepsilon\rho_{\mathrm{f}}C_{\mathrm{f}}}{h_0a_0},$$

$$HCR=\frac{\rho_{\mathrm{f}}C_{\mathrm{f}}\varepsilon}{(1-\varepsilon)\rho_{\mathrm{s}}C_{\mathrm{s}}}.$$

where T_h is the inlet temperature of fluid for charging, while T_c is that for discharging.

For the discharging process, the initial condition is given by,

$$t^* = 0: \ \theta_s = \theta_f = f_0(z^*), \tag{10}$$

where $f_0(z^*)$ is the initial dimensionless temperature distributions. The boundary conditions are,

$$z^* = 0: \ \theta_f = 0, \ \frac{d\theta_s}{dz} = 0. \tag{11}$$

Solving Eqs. (8) and (9) with the corresponding initial and boundary conditions Eqs. (10) and (11) derives the predictive model for the temperature of fluid and solid during the discharging process. Due to the symmetry between discharging and charging processes [10], the discharge model can also be employed to predict the charging behavior by the transform of two variables θ and z^* as below,

$$\theta_c = 1 - \theta_d, \qquad z_c^* = 1 - z^*{}_d. \tag{12}$$

3 Problem Solution

The Laplace transform can be used to solve the equations above. The Laplace transform of dimensionless temperature is expressed as,

$$\tilde{\theta}_f(s) = \int_0^\infty \theta_f(t)\exp(-st)dt\,,$$
$$\tilde{\theta}_s(s) = \int_0^\infty \theta_s(t)\exp(-st)dt\,. \tag{13}$$

Then, Eqs. (8) and (9) are transformed to,

$$s\tilde{\theta}_f - f_0 = \frac{1}{\tau_{fs}}\left(\tilde{\theta}_s - \tilde{\theta}_f\right) - \frac{U}{\overline{U}}\frac{\partial\tilde{\theta}_f}{\partial z^*} + \frac{1}{\tau_0}\left(\frac{\theta_0}{s} - \tilde{\theta}_f\right), \tag{14}$$

$$s\tilde{\theta}_s - f_0 = -\frac{\mathrm{HCR}}{\tau_{fs}}\left(\tilde{\theta}_s - \tilde{\theta}_f\right) - \frac{\mathrm{HCR}}{\tau_0}\left(\tilde{\theta}_s - \frac{\theta_0}{s}\right). \tag{15}$$

Solving Eqs. (14) and (15) gives the analytical models of $\tilde{\theta}_f$ and $\tilde{\theta}_s$,

$$\tilde{\theta}_f(s, z^*) = \int_0^{z^*} \exp\left(-\int_\xi^{z^*} P_f\, d\eta\right)\left[Q_{f1}\theta_0 + Q_{f2}f_0(\xi)\right]d\xi\,, \tag{16}$$

$$\tilde{\theta}_f(s, z^*) = \frac{\frac{\mathrm{HCR}}{\tau_{fs}}\tilde{\theta}_f(s) + \frac{\mathrm{HCR}}{\tau_0}\frac{\theta_0}{s} + f_0(z^*)}{s + \mathrm{HCR}\left(\frac{1}{\tau_{fs}} + \frac{1}{\tau_0}\right)}. \tag{17}$$

with

$$P_f = \frac{\overline{U}}{U}\left[s + \frac{1}{\tau_{fs}} + \frac{1}{\tau_0} - \frac{1}{\tau_{fs}}\frac{\frac{\mathrm{HCR}}{\tau_{fs}}}{s + \mathrm{HCR}\left(\frac{1}{\tau_{fs}} + \frac{1}{\tau_0}\right)}\right],$$

$$Q_{f1} = \frac{\overline{U}}{U}\frac{1}{s}\left[\frac{1}{\tau_{fs}}\frac{\frac{\mathrm{HCR}}{\tau_0}}{s + \mathrm{HCR}\left(\frac{1}{\tau_{fs}} + \frac{1}{\tau_0}\right)} + \frac{1}{\tau_0}\right],$$

$$Q_{f2} = \frac{\overline{U}}{U}\left[1 + \frac{1}{\tau_{fs}}\frac{1}{s + \mathrm{HCR}\left(\frac{1}{\tau_{fs}} + \frac{1}{\tau_0}\right)}\right].$$

The analysis on the influence of filler porosity's non-uniform distributions on the thermal performance of the storage tank are conducted using the analytical model above.

4 Results and Discussions

The performance of a specific heat storage tank is usually characterized by the discharging (η_{disch}) and charging (η_{ch}) efficiencies [5],

$$\eta_d = \frac{\int_0^{t_{d80\%}} \dot{m}C_f\{T_{f,out}(t) - T_c\}dt}{\int_0^{t_{c20\%}} \dot{m}C_f\{T_h - T_c\}dt}, \tag{18}$$

$$\eta_c = \frac{\int_0^{t_{c20\%}} \dot{m}C_f\{T_h - T_{f,out}(t)\}dt}{\int_0^{t_{c20\%}} \dot{m}C_f\{T_h - T_c\}dt}. \tag{19}$$

where $t_{c20\%}$ is the cut-off time for charging as the outlet temperature of fluid reaches 20% of the temperature difference ($T_h - T_c$), and $t_{d80\%}$ is the the cut-off time for discharging as the outlet temperature of fluid decreases to 80% of the temperature difference ($T_h - T_c$). Due to the symmetry between discharging and charging, $t_{c20\%}$ should be equal to $t_{d80\%}$.

Following the identical manner to convert Eqs. (18) and (19) to dimensionless, we have

$$\eta_d = \int_0^{t^*_{d80\%}} \theta_{f,out}dt^* = \eta_c. \tag{20}$$

In this sense, we only need to analyze the outlet temperature of fluid, $\theta_{f,out}$, during discharging for evaluating the influence of different filler's porosity distributions on both the charging and discharging efficiencies.

In the numerical experiments, the parameters setting is as follows: average porosity $\bar{\varepsilon} = 0.5$, tank height $H = 2\,\mathrm{m}$, tank radius $R = 2\,\mathrm{m}$, equivalent diameter of solid particles $d = 0.01\,\mathrm{m}$, mass flow rate $\dot{m} = 2\,\mathrm{kg/s}$, and $T_c = T_0$. Moreover, the properties of fluid (solar salt) and filler material (quartzite) are given in Tab.1 referring to Ref. [6].

Tab.1 Properties of fluid and filler material [6]

Material	Density kg/m^3	Specific heat J/kg-K	Dynamic viscosity kg/m-s	Thermal conductivity W/m-K
Solar salt	1899	1495	0.00326	0.57
Quartzite rock	2640	1050	N/A	2.8

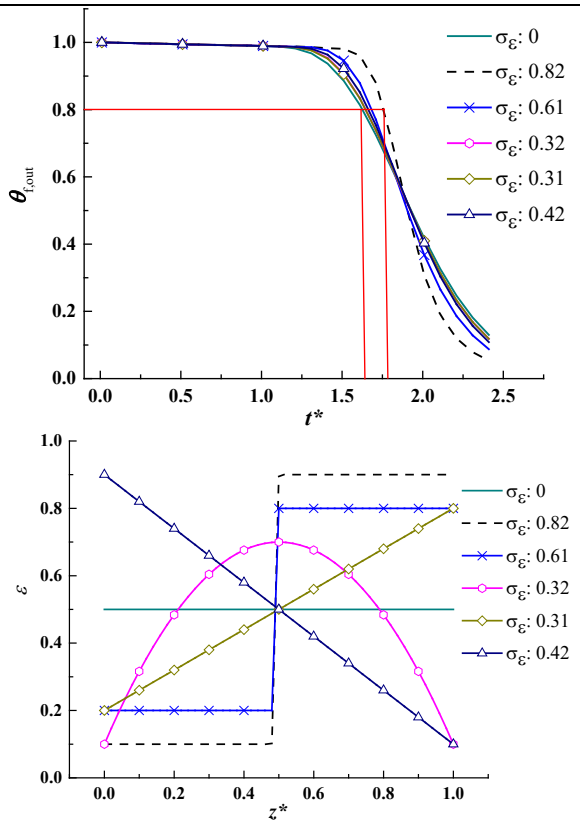

Fig. 2 (a) Outlet temperature of fluid varying with time; (b) Varied porosity distributions along z*.

According to Fig.2, even when the total amount of filler material, that is, the integration of porosity, is prescribed, the varied porosity distributions can lead to the different behaviors of outlet temperature. Furthermore, in order to evaluate the degree of non-uniformity, the standard variation of porosity along the axil direction is calculated,

$$\sigma_\varepsilon = \frac{\sqrt{\int_0^1 (\varepsilon(z) - \bar{\varepsilon})^2 dz^*}}{\bar{\varepsilon}}. \qquad (21)$$

Apparently, the non-uniformity increases with the increasing σ_ε. Fig.2 shows that the cut-off time $t_{d80\%}$ for discharging increases as the non-uniformity, i.e., σ_ε, is enhanced. A bigger $t_{d80\%}$ means a longer valid discharging process, since the outlet temperature of HTF can maintain at the high temperature during a longer time range. Thus, the thermal performance of the storage tank is improved as well.

4 Conclusion

In the present work, the analytical model for characterizing the transient thermal transport process within the packed-bed sensible heat thermocline storage tanks with a height-dependent filler porosity is derived using the Laplace transform. The analyses based on the models indicate that the different porosity distributions can result in the significantly-different behaviors of outlet temperature and thus the varied charging and discharging efficiencies, when the total amount of filler materials is fixed, and the thermal performance will be improved with the increasing non-uniformity of filler porosity distributions. Our work may provide a new way to optimize the thermocline storage tanks in practice.

References:

[1] Tian Y, Zhao CY. A review of solar collectors and thermal energy storage in solar thermal applications. *Appl Energy* 2013;104:538–53.

[2] Pelay U, Luo L, Fan Y, Stitou D, Rood M. Thermal energy storage systems for concentrated solar power plants. *Renew Sustain Energy Rev* 2017;79:82–100.

[3] PELAY U, LUO L, FAN Y, STITOU D. Dynamic modeling and simulation of a concentrating solar power plant integrated with a thermochemical energy storage system. *J Energy Storage* 2020;28:101164..

[4] Lou W, Fan Y, Luo L. Single-tank thermal energy storage systems for concentrated solar power: Flow distribution optimization for thermocline evolution management. *J Energy Storage* 2020;32:101749.

[5] Lou W, Luo L, Hua Y, Fan Y, Du Z. A review on the performance indicators and influencing factors for the thermocline thermal energy storage systems. *Energies* 2021;14:1–19.

[6] Reddy KS, Jawahar V, Sivakumar S, Mallick TK. Performance investigation of single-tank

thermocline storage systems for CSP plants. *Sol Energy* 2017;144:740–9.

[7] López Sanz J, Cabello Nuñez F, Zaversky F. Benchmarking analysis of a novel thermocline hybrid thermal energy storage system using steelmaking slag pebbles as packed-bed filler material for central receiver applications. *Sol Energy* 2019;188:644–54.

[8] Hua Y-C, Zhao T, Guo Z-Y. Transient thermal conduction optimization for solid sensible heat thermal energy storage modules by the Monte Carlo method. *Energy* 2017;133:338–47.

[9] Van Lew JT, Li P, Chan CL, Karaki W, Stephens J. Analysis of heat storage and delivery of a thermocline tank having solid filler material. *J Sol Energy Eng Trans ASME* 2011;133:1–10.

[10] Karaki W, Van Lew JT, Li P, Chan CL, Stephens J. Heat transfer in thermocline storage system with filler materials: Analytical model. *ASME 2010 4th Int. Conf. Energy Sustain. ES* 2010, vol. 2, 2010, p. 725–34.

Contribution of individual authors to the creation of a scientific article (ghostwriting policy)

Yuchao HUA carried out the mathematic derivation and the simulation, and wrote the draft.
Lingai Luo was responsible for the supervision and polishing the manuscript.

Sources of funding for research presented in a scientific article or scientific article itself

This work is financially supported by Région Pays de la Loire France within the NExT2Talents program TOP-OPTIM project (998UMR6607 EOTP NEXINTERTALENTHUA), and by the French ANR within the project OPTICLINE (ANR-17-CE06–0013).

Creative Commons Attribution License 4.0 (Attribution 4.0 International , CC BY 4.0)